JOURNAL OF MATERIALS SCIENCE 30 (1995) 2377–2381

Effect of composition, film thickness and annealing on the optical properties of Bi–Sb–Se thin films

M. FADEL, M. M. EL-SAMANOUDY
Physics Department, Faculty of Education, Ain Shams University, Cairo, Egypt
K. A. SHARAF
Physics Department, Faculty of Science (Girls), Al-Azhar University, Cairo, Egypt

Thin films of $Bi_{10}Sb_xSe_{90-x}$ ($x \geq 35, 40, 45$) of different composition and thickness, were deposited on glass substrates by vacuum evaporation. Optical absorption measurements show that the fundamental absorption edge is a function of glass composition, film thickness and annealing temperature. The optical absorption is due to indirect electronic transitions. The value of the optical band gap was found to increase with thickness and decreasing the antimony content and with increasing temperature of heat treatment. The validity of the Urbach rule was investigated and the respective parameters estimated. X-ray diffraction was used to obtain an insight into the structural information.

1. Introduction

Chalcogenide glasses have been attracting much attention in the fields of electronics as well as infrared optics, because they exhibit several peculiar phenomena applicable for devices such as electrical switches and memories [1, 2] and photoresists [3].

Chalcogenide thin films have been extensively studied [4–7]. The use of these films for reversible optical recording by the amorphous crystalline phase change has recently been reported [8–10]. The chalcogenide used for the recording medium must be easy to amorphize and crystallize. It was reported [11] that the addition of bismuth to selenium facilitates crystallization.

Glassy chalcogenide semiconductors show great variations in band gap values which are influenced by the variation on the composition of such materials [12–15].

2. Experimental procedure

The system under investigation, $Bi_{10}Sb_xSe_{90-x}$ ($x \geq 35, 40, 45$) were prepared from commercial elements from the Balzers company having high-purity (99.999%) bismuth, antimony and selenium in appropriate atomic percentages; proportions were weighed using an electric balance and sealed in an evacuated silica tube under a vacuum of 10^{-5} torr (1 torr = 133.322 Pa). The tube was kept in a furnace at 1000 °C for 72 h. Synthesis was accomplished in an oscillatory furnace designed to ensure homogeneity. The tube was rapidly quenched in ice-cold water. After removing the ingot from the ampoule, it was used to fabricate thin-film samples.

Thin evaporated films of $Bi_{10}Sb_xSe_{90-x}$ ($x \geq 35, 40, 45$) of different compositions were deposited at room temperature by thermal evaporation on to clean quartz substrates held at partial pressure of the order of 10^{-5} torr. The accurate thickness of the films was measured by an interferometric method.

Annealing was carried out at a particular temperature from room temperature to 423 K. Measurements were made after cooling the films to room temperature. Absorption measurements in the wavelength range 350–900 nm were carried out using a Varian DMS 100S spectrophotometer.

The present work was concerned with some experimental observations on the effects of composition, heat treatment and thickness variation on the optical properties of $Bi_{10}Sb_xSe_{90-x}$ thin films.

3. Results and discussion

3.1. X-ray diffraction of $Bi_{10}Sb_xSe_{90-x}$

X-ray diffraction (XRD) patterns were measured in order to understand the structural changes produced in $Bi_{10}Sb_{35}Se_{55}$, $Bi_{10}Sb_{40}Se_{50}$ and $Bi_{10}Sb_{45}Se_{35}$ thin films having different composition, thicknesses and by heat treatment at different elevated temperatures.

Fig. 1a shows the X-ray diffraction patterns of three different compositions of the chalcogenide glass system $Bi_{10}Sb_xSe_{90-x}$. It is clear from these patterns that no sharp diffraction lines are present. Fig. 1b shows the X-ray diffraction patterns of films of the glass system $Bi_{10}Sb_{40}Se_{50}$ having different thicknesses. It is clear from these patterns that no sharp diffraction lines are present. This indicates the amorphous state,

0022–2461

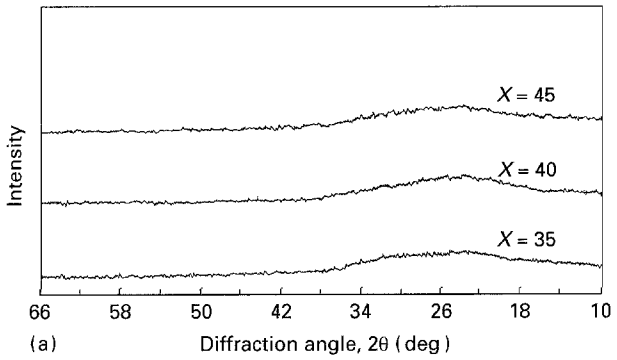

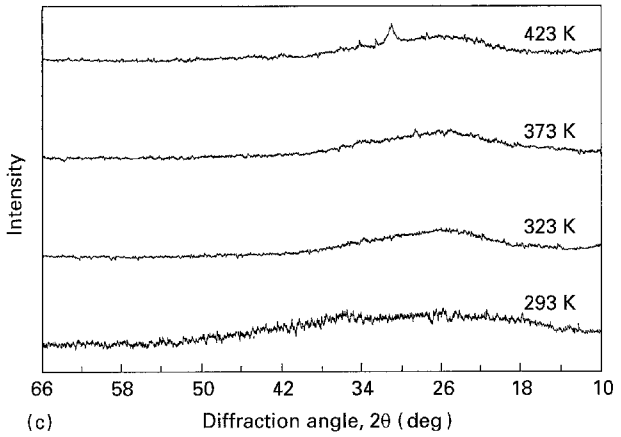

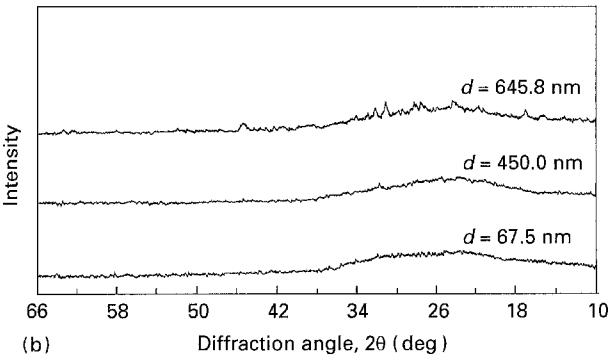

Figure 1 X-ray diffraction patterns of (a) $Bi_{10}Sb_xSe_{90-x}$ glass samples having different composition, (b) $Bi_{10}Sb_{40}Se_{50}$ having different thicknesses, and (c) glass samples of $Bi_{10}Sb_{45}Se_{45}$ annealed at different temperatures.

but at a thickness of 645.8 nm, small traces of peaks are observed due to a phase transition. From Fig. 1c it is revealed that the films of composition $Bi_{10}Sb_{45}Se_{45}$ both as-deposited and annealed at 323 and 373 K are non-crystalline. The grain size of the films was so small and the disorder within these grains so high that no specific diffraction peaks could be detected. Slight traces of peaks are observed for films annealed at 423 K for 2 h, which indicates some amorphous to crystalline transition as a result of heat treatment at 423 K.

3.2. Optical absorption

The measurement of optical absorption and particularly the absorption edge is important especially in connection with the theory of the electronic structure of amorphous materials. In the high absorption region, Tauc *et al.* [16] and Davis and Mott [17] independently derived an expression relating the absorption coefficient $\alpha(\omega)$, to photon energy, $\hbar\omega$

$$\alpha(\omega) = \beta(\hbar\omega - E_{opt})^M/\hbar\omega \quad (1)$$

where β is a constant $(4\pi\sigma_0/ncE_e)$, where c is the speed of light, σ_0 is the extrapolated d.c. conductivity at $T = \infty$, E_e is a measure of the extent of band-tailing, n is the refractive index, E_{opt} is the optical energy gap, and M is a number which characterizes the optical absorption process: $M = 1/2$ for a direct allowed transition, $M = 3/2$ for a direct forbidden transition, $M = 2$ for an indirect allowed transition and $M = 3$ for an indirect forbidden transition.

Absorption at lower photon energy usually follows the Urbach rule [18], i.e.

$$\alpha(\omega) = \alpha_0 \exp \hbar\omega/E_e \quad (2)$$

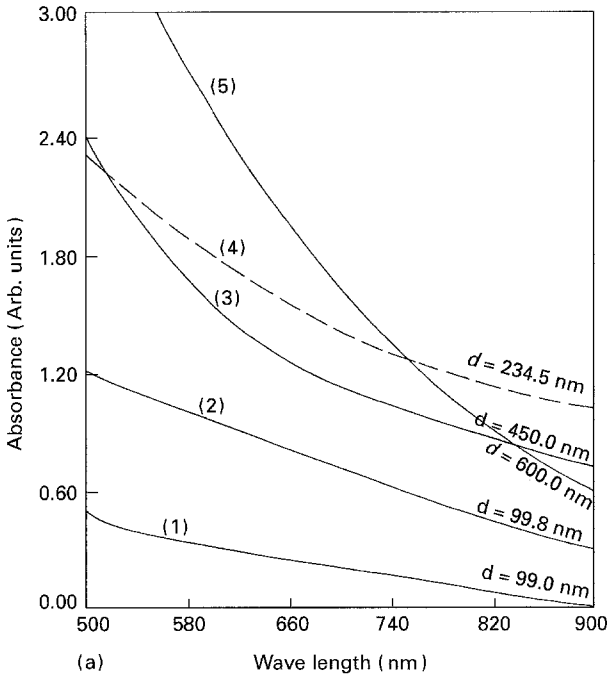

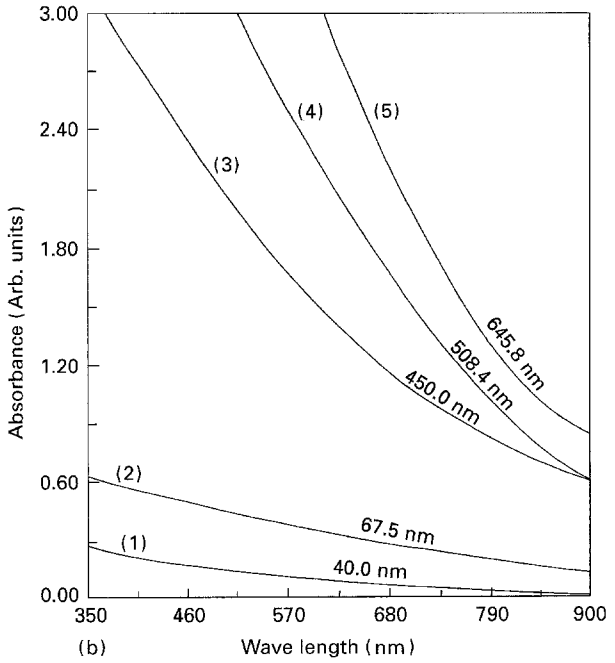

Figure 2 Absorption spectra as a function of wavelength for $Bi_{10}Sb_xSe_{90-x}$ thin films having different composition and thickness: (a) $Bi_{10}Sb_{35}Se_{55}$ (curves 1, 2 and 5) and $Bi_{10}Sb_{45}Se_{45}$ (curves 2 and 4); (b) $Bi_{10}Sb_{40}Se_{50}$ having different thickness.

where E_e is the Urbach energy which is interpreted as the width of the tails of localized states in the band gap.

The optical absorbance as a function of wavelength for samples having different compositions and thickness is shown in Fig. 2a and b, respectively. It can be seen that the position of the fundamental absorption edge shifts to the higher wavelength region with increasing antimony content and increasing film thickness.

The graph of $(\alpha\hbar\omega)^{1/2}$ versus $(\hbar\omega)$ (Fig. 3a, b) has a well-defined linear region thus confirming that Equation 1 is obeyed; values of E_{opt} and β are given in Table I.

Fig. 4a and b demonstrates that the exponential behaviour of the absorption edge, via Equation 2, is satisfied in $Bi_{10}Sb_xSe_{90-x}$ chalcogenide glasses. Values of the width, E_e, of the band tails are also listed in Table I. The values of E_e are very much larger than 0.05 eV and vary with composition. The Tauc model [19] based on electronic transitions between localized states in the band edge tails may well be valid in these glasses. The observed decrease in the optical gap, E_{opt}, with added antimony can be explained by the increased tailing [20] of the conduction band edge into the gap, due to the addition of antimony.

The effect of film thickness on E_{opt} can be seen in Table I, and the optical gap increases with increasing thickness of $Bi_{10}Sb_xSe_{90-x}$ ($x \geq 35, 40, 45$) thin films. This variation may be explained as due to the presence of defects in amorphous materials as for a-$I_{0.4}Se_{0.6}$ films [21], in terms of the elimination of defects in the amorphous structure. The insufficient number of atoms deposited in the amorphous film results in the

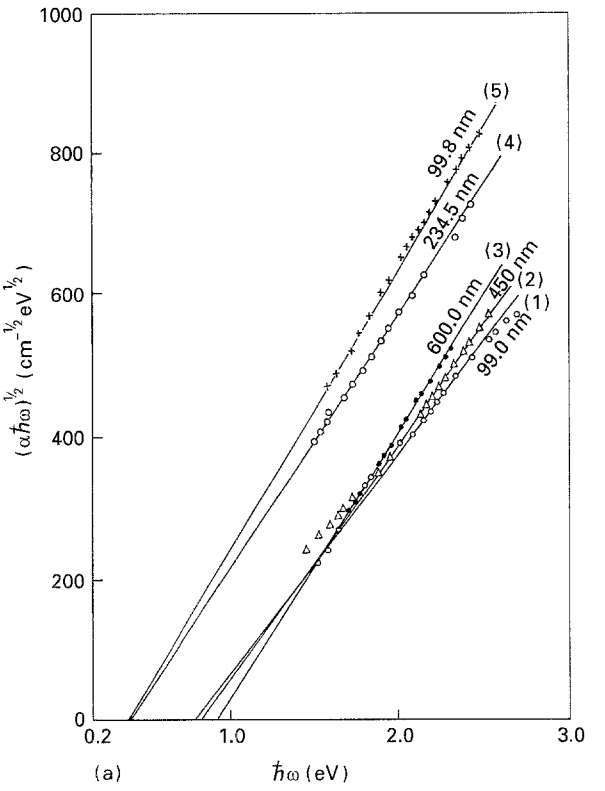

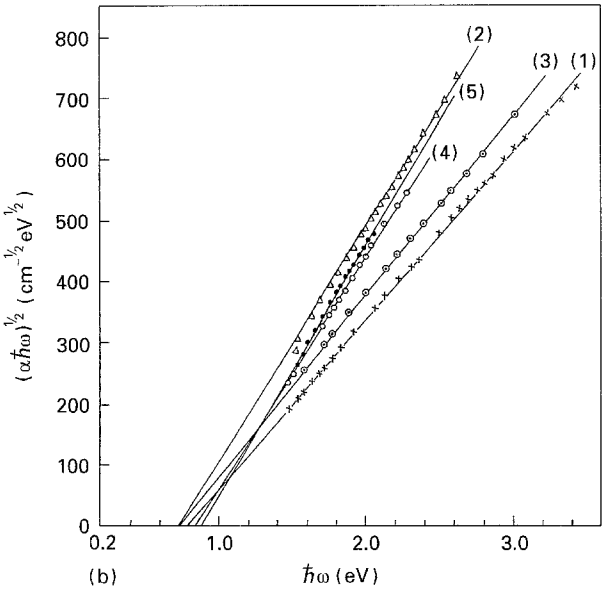

Figure 3 Optical absorption data of Fig. 2 replotted in accordance with absorption by indirect transition. (a) $Bi_{10}Sb_{35}Se_{55}$, curves 1–3 and $Bi_{10}Sb_{45}Se_{45}$, curves 4 and 5. (b) $Bi_{10}Sb_{40}Se_{50}$ thin films at different thicknesses: (1) 40.0 nm, (2) 67.5 nm, (3) 450.0 nm, (4) 508.4 nm, (5) 645.8 nm.

TABLE I The optical properties of $Bi_{10}Sb_xSe_{90-x}$ of different compositions and thickness

Composition	Thickness (nm)	E_{opt}/ (eV)	E_e/ (eV)	$\beta(10^5\,cm^{-1}eV^{-1})$
$Bi_{10}Sb_{35}Se_{55}$	99.0	0.78	0.444	1.003
	450.0	0.84	0.555	1.314
	600.0	0.96	0.417	1.406
$Bi_{10}Sb_{40}Se_{50}$	40.0	0.80	0.480	0.803
	67.5	0.72	0.415	1.534
	450.0	0.74	0.667	0.850
	645.8	0.83	0.360	1.502
	–	0.88	0.550	1.502
$Bi_{10}Sb_{45}Se_{45}$	99.80	0.38	0.588	1.650
	234.5	0.40	1.070	1.284

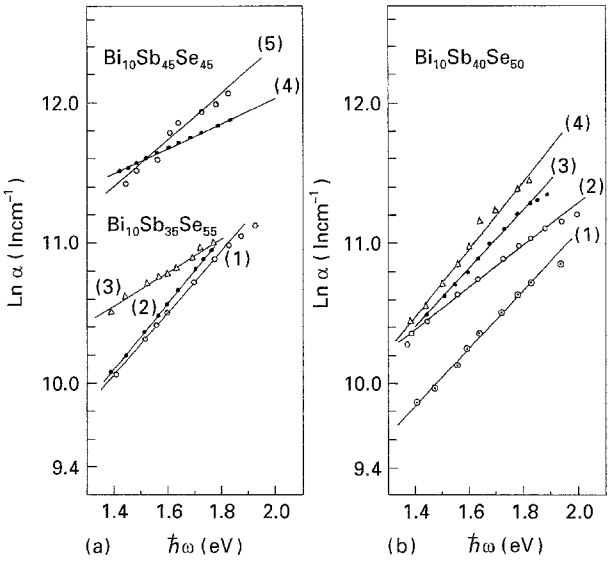

Figure 4 Data of Fig. 2 replotted in accordance with the Urbach rule. (a) $Bi_{10}Sb_{35}Se_{55}$, curves 1–3: (1) 99.0 nm, (2) 600.0 nm, (3) 450.0 nm; $Bi_{10}Sb_{45}Se_{45}$, curves 4 and 5: (4) 234.5 nm (5) 99.8 nm. (b) $Bi_{10}Sb_{40}Se_{50}$. Curves 1–4; (1) 40.0 nm, (2) 450.0 nm, (3) 645.8 nm, (4) 67.5 nm.

existence of unsaturated bonds [22]. The unsaturated bonds are responsible for the formation of some defects in the films which produce localized states in amorphous solids [23]. Thicker films are characterized by a more homogenous network, which minimizes the number of defects and the localized states, and thus the optical gap increases. These results are in good agreement with these obtained for Bi_2Te_2Se thin films [4].

The absorbances of the as-deposited and annealed $Bi_{10}Sb_xSe_{90-x}$ thin films are shown in Fig. 5a and b. The curves are shown to be identical in character, but they shift to longer wavelength with increasing annealing temperature, and so the values of E_{opt}, in general, decrease (Fig. 6). The increase in the absorbance value of the chalcogenide films after annealing can be related to some transformation from a glassy structure to a more crystalline phase. The calculated values of E_{opt} and E_e from Fig. 7 are listed in Table II.

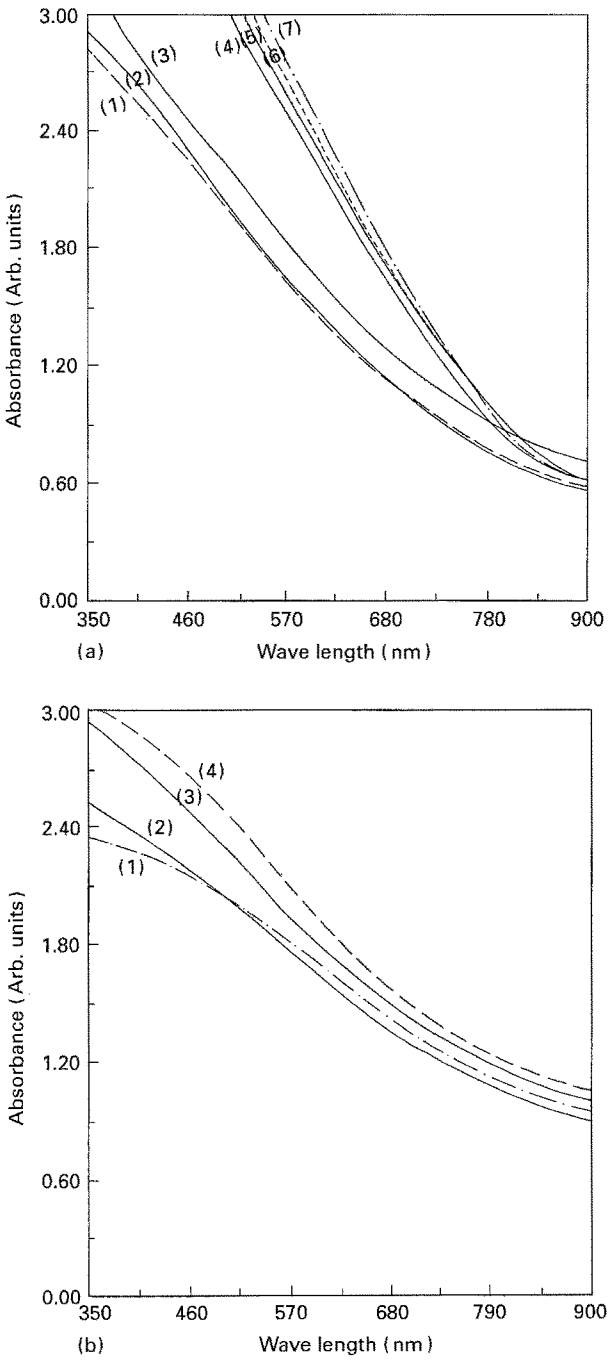

Figure 5 Optical absorption spectra of annealed $Bi_{10}Sb_xSe_{90-x}$ thin films. (a) $Bi_{10}Sb_{40}Se_{50}$, thickness 450 nm, curves 1–3: (1) 323 K, (2) 373 K, (3) 423 K; $Bi_{10}Sb_{35}Se_{55}$, thickness 600.0 nm, curves 4–7: (4) 373 K, (5) 323 K, (6) 298 K and (7) 423 K. (b) $Bi_{10}Sb_{45}Se_{45}$, thickness 234.5 nm, curves 1–4: (1) 373 K, (2) 323 K, (3) 298 K and (4) 423 K.

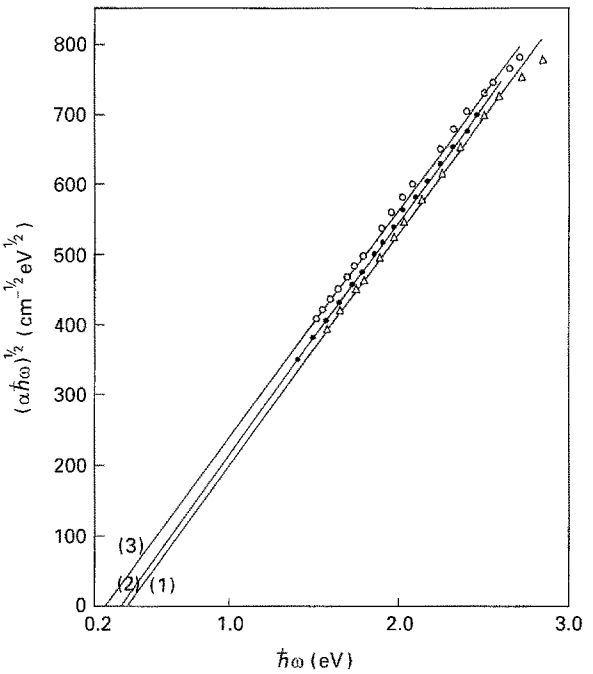

Figure 6 Data of Fig. 5b replotted in accordance with the theory of indirect transitions. Curves 1–3: (1) 323 K, (2) 373 K and (3) 423 K.

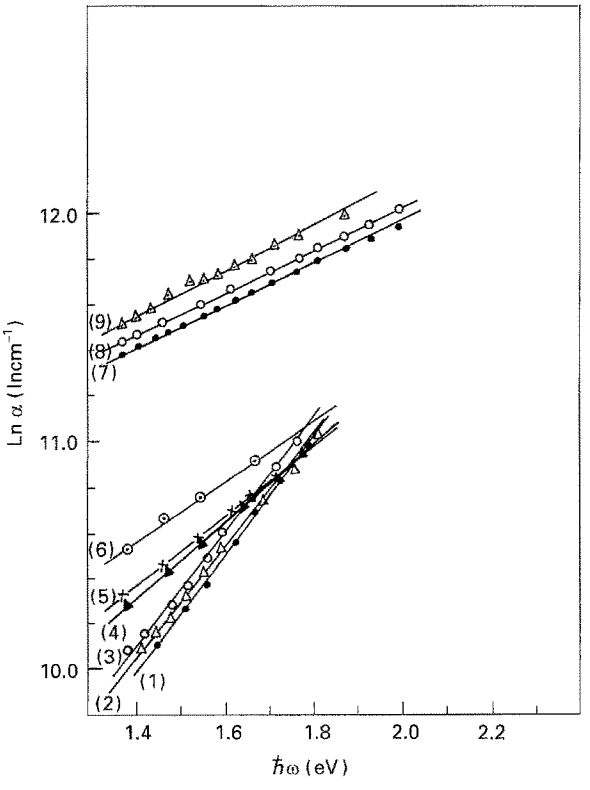

Figure 7 Data of Fig. 5 replotted in accordance with the Urbach rule, (a) $Bi_{10}Sb_{35}Se_{55}$, thickness 600.0 nm, curves 1–3, for temperatures 323, 373 and 423 K. (b) $Bi_{10}Sb_{40}Se_{50}$, thickness 450.0 nm, curves 4–6, at annealing temperatures 373, 323 and 423 K, respectively. (c) $Bi_{10}Sb_{45}Se_{45}$, thickness 234.5 nm, curves 7–9 at annealing temperatures 323, 373 and 423 K.

TABLE II The effect of heat treatment on the optical properties of $Bi_{10}Sb_xSe_{90-x}$

Composition	Temperature (K)		Thickness (nm)	E_{opt}/ (eV)	E_e/ (eV)	$\beta(10^5\,cm^{-1}eV^{-1})$
$Bi_{10}Sb_{35}Se_{55}$	293	600.0	0.96	0.417		1.4063
	323		0.92	0.413		1.269
	373		0.92	0.413		1.269
	423		0.86	0.414		1.097
$Bi_{10}Sb_{40}Se_{50}$	293	450.0	0.74	0.667		0.850
	323		0.68	0.592		0.834
	373		0.65	0.671		0.803
	423		0.57	0.775		0.711
$Bi_{10}Sb_{45}Se_{45}$	293	234.5	0.40	1.07		1.284
	323		0.40	1.05		1.111
	373		0.36	1.05		1.110
	423		0.26	1.10		1.140

A decrease in the optical band gap of the amorphous films can be caused by the increased tailing of the conduction band edge into the gap due to environmental contamination during heat treatments [25]. On the other hand, the growth of the crystallization phases with increasing annealing temperature can lead to an increase in the optical band gap. In the present work, the observed decrease in the optical band gap after heat treatment can be interpreted by the higher effect of the environmental contaminations over that of the crystallization phases on the optical properties of $Bi_{10}Sb_xSe_{90-x}$ chalcogenide films.

4. Conclusion

Increasing the molar percentage of antimony caused an increase in the disorder of the system under investigation. This caused the defect or localized states to extend further into the band gap. The optical parameters, E_{opt}, β, and E_e, are affected by both film thickness and annealing temperature. This confirms the effect of these two factors on the density of localized states.

References

1. S. R. OVSHINSKY, *Phys. Rev. Lett.* **21** (1968) 1450.
2. H. FRITZSCHE and S. R. OVSHINSKY, *J. Non-Cryst. Solids* **2** (1970) 148.
3. H. NAGAL, A. YOSHIKAWA, Y. TOYOSHIMA, O. OCHI and Y. MIZVSHIMA, *Appl. Phys. Lett.* **28** (1976) 145.
4. M. M. EL-SAMANOUDY and M. FADEL, *J. Mater. Sci.* **27** (1992) 646.
5. H. H. LABIB, A. Y. MORSY, S. S. FOUAD, H. S. METWALLY, M. F. ABDEL-AAL, M. A. AFIFI and A. A. EL-SHAZLY, *J. Mater. Sci. Lett.* **8** (1989) 1244.
6. Y. SRIPATHI, G. B. REDDY, L. K. MALHOTRA, *J. Mater. Sci. Mater. Electron.* **3** (1992) 164
7. R. MATHUR and A. KUMAR, *Solid State Commun.* **61** (1987) 785.
8. P. F. CARCIA, F. D. KALK, P. E. BIERSTEDT, A. FERRETTI, G. A. JONES and D. G. SWARIZ: FAGER, *J. Appl. Phys.* **64** (1988) 1671.
9. Y. MAEDA, H. ANDOH, I. IKUTA and H. MINEMURA, *J. Appl. Phys.* **64** (1988) 1715.
10. K. A. RUBIN and M. CHEN, *Thin Solid Films* **181** (1989) 129.
11. A. MUNOZ, F. L. CUMBRERA and R. MARAVEZ, *ibid.* **186** (1990) 37.
12. M. SUZUKI, H. OHDAIRA, T. MATSUMI, M. KUMEDA and T. SCHIMIZU, *Jpn J. Appl. Phys.* **16** (1977) 221.
13. N. TOHGE, T. MINAMI and M. TANAKA, *J. Non-Cryst. Solids* **37** (1980) 23.
14. N. TOHGE, T. MINAMI, Y. YAMAMOTO and M. TANAKA, *J. Appl. Phys.* **51** (1980) 1048.
15. M. SZUKWEI, Y. HANMEI and C. ZONGCAI, *J. Non-Cryst. Solids* **52** (1982) 181.
16. J. TAUC, R. GRIGOROVICI and A. VANCU, *Phys. Status Solidi* **15** (1966) 627.
17. E. A. DAVIS and N. F. MOTT, *Philos. Mag.* **22** (1970) 903.
18. F. URBACH, *Phys. Rev.* **92** (1953) 1324.
19. J. TAUC, "The Optical Properties of Solids", edited by F. Abeles (North Holland, Amsterdam, 1970) p. 227.
20. P. NAGEL, L. TICHY, A. TRISKA and H. TICHA, *J. Non-Cryst. Solids* **59/60** (1983) 1015.
21. S. CHAUDHURI, S. K. BISWAS and A. CHOUDHURY, *J. Mater. Sci.* **23** (1988) 4470.
22. S. K. BISWAS, S. CHAUDHURI and A. CHOUDHURY, *Phys. Status. Solidi (a)* **105** (1988) 467.
23. K. I. ARSHAK and C. A. HOGARTH, *Thin Solid Films* **137** (1986) 281.
24. E. K. SHOKRER, M. M. WAKKAD, *J. Mater. Sci.* **27** (1992) 1197.
25. P. NAGELS, I. TICHY, A. TRISKA and H. TICHA, *J. Non-Cryst. Solids* **59/60** (1983) 1015.

Received 28 September 1993
and accepted 31 October 1994